Pyrostegia venusta heptane extract containing saturated aliphatic hydrocarbons induces apoptosis on B16F10-Nex2 melanoma cells and displays antitumor activity *in vivo*

Carlos R. Figueiredo, Alisson L. Matsuo, Felipe V. Pereira, Aline N. Rabaça, Camyla F. Farias, Natália Girola, Mariana H. Massaoka, Ricardo A. Azevedo, Jorge A.B. Scutti, Denise C. Arruda, Luciana P. Silva[1], Elaine G. Rodrigues, João Henrique G. Lago[2], Luiz R. Travassos, Regildo M.G. Silva[1]

Departments of Microbiology, Immunology and Parasitology, Cell Biology Division and Experimental Oncology Unit (UNONEX), Federal University of São Paulo (UNIFESP), São Paulo, SP, [1]Department of Biological Sciences, Phytochemistry Laboratory. Universidade Estadual Paulista (UNESP), Assis, São Paulo State, [2]Institute of Environmental, Chemical and Pharmaceutical Sciences, Federal University of São Paulo (UNIFESP), Diadema, São Paulo, Brazil

Submitted: 19-08-2013 Revised: 25-09-2013 Published: 28-05-2014

ABSTRACT

Background: *Pyrostegia venusta* (Ker. Gawl.) Miers (Bignoniacea) is a medicinal plant from the Brazilian Cerrado used to treat leucoderma and common diseases of the respiratory system. **Objective:** To investigate the antitumor activity of *P.venusta* extracts against melanoma. **Materials and Methods:** The cytotoxic activity and tumor induced cell death of heptane extract (HE) from *P. venusta* flowers was evaluated against murine melanoma B16F10-Nex2 cells *in vitro* and in a syngeneic model *in vivo*. **Results:** We found that HE induced apoptosis in melanoma cells by disruption of the mitochondrial membrane potential, induction of reactive oxygen species and late apoptosis evidenced by plasma membrane blebbing, cell shrinkage, chromatin condensation and DNA fragmentation, exposure of phosphatidylserine on the cell surface and activation of caspase-2,-3,-8,-9. HE was also protective against singeneyc subcutaneous melanoma HE compounds were also able to induce cell cycle arrest at G2/M phases on tumor cells. On fractionation of HE in silica gel we isolated a cytotoxic fraction that contained a mixture of saturated hydrocarbons identified by ^{1}H NMR and GC-MS analyses. Predominant species were octacosane ($C_{28}H_{58}$-36%) and triacontane ($C_{30}H_{62}$-13%), which individually showed significant cytotoxic activity against murine melanoma B16F10-Nex2 cells *in vitro* and a very promising antitumor protection against subcutaneous melanoma *in vivo*. **Conclusion:** The results suggest that the components of the heptane extract, mainly octasane and triacontane, which showed antitumor properties in experimental melanoma upon regional administration, might also be therapeutic in human cancer, such as in the mostly epidermal and slowly invasive melanomas, such as acral lentiginous melanoma, as an adjuvant treatment to surgical excision.

Key words: Apoptosis, cytotoxicity, melanoma, *Pyrostegia venusta,* saturated hydrocarbons

Access this article online

Website: www.phcog.com

DOI: 10.4103/0973-1296.133284

Quick Response Code:

INTRODUCTION

Malignant melanoma is a very aggressive form of skin cancer, with a mortality rate that has increased in 2% annually since 1960, making it a worldwide public health risk and the fastest growing of all cancer types.[1] Melanomas are usually removed by resection but are very difficult to cure in the metastatic form. Several strategies and combinations of anticancer drugs have been used in an effort to improve the therapeutic effect on malignant melanomas.[2] Solid tumor cells develop resistance to antineoplasic drugs and multidrug resistance is a major cause of chemotherapy failures of human cancer.[3]

Among skin cancers, the acral lentiginous melanoma (ALM) is a variant occurring on volar surfaces of hands, feet, subungual site, fingers or toes and is characterized by slow

Address for correspondence:
Dr. Carlos R. Figueiredo, Department of Microbiology, Immunology and Parasitology, Experimental Oncology Unit (UNONEX), Federal University of São Paulo (UNIFESP). Rua Botucatu 862, 8º andar, Vila Clementino, São Paulo, SP 04023-062, Brazil.
E-mail: c.figueiredo@unifesp.br

lentiginous radial growth, with heavily pigmented tumor cells with diffuse reticular infiltration, lesions becoming unusually large, thick and ulcerated.[4] Acral melanoma poses a challenge to clinicians who must balance adequate oncologic resection with preservation of limb function.[5] In alternative to surgical intervention or to aid in the reduction of tumor size, the development of chemotherapy agents against this malignant melanoma is highly justified.

A frequently utilized syngeneic murine model of melanoma is that of B16F10 cell line in C57Bl/6 mice and the F10 subline, isolated by I.J.Fidler, is most invasive and virulent.[6] Therefore, it is chosen to monitor the *in vitro* and *in vivo* activity of anti-melanoma agents causing cell death or cytostatic effects. Cell death can occur by several mechanisms such as necrosis, autophagy, apoptosis, cornification and many other atypical cell death modalities.[7] Programmed cell death by apoptosis is a major natural barrier to cancer development.[8]

On testing new antitumor molecules, apoptosis is primarily looked for as a relevant cell toxicity pathway. An important function of apoptosis is to eliminate preneoplastic and neoplastic cells.[9] As opposed to necrosis, apoptosis progresses through a series of well-defined morphological and biochemical stages that occur in the nucleus as well as in the mitochondria and cytoplasm of the dying cell.[10] Apoptosis involves a series of biochemical events, including blebbing, cell shrinkage, mitochondria permeability, nuclear fragmentation, chromatin condensation and fragmentation.[11] Added to these features, caspase proteolytic activity is a hallmark of apoptosis.[12] Cancer cells may adapt to the oncogenic signaling by disabling their senescence-or apoptosis-inducing pathways.[13] The induction of a pro-apoptotic therapy is therefore of interest because this mechanism of cell control is deregulated in tumor cells.[14] Unlike necrosis, apoptosis is a cell death process that results in the elimination of cellular debris without damage to tissues, because phagocytic cells engulf apoptotic cells without promoting tissue inflammation as observed in necrosis.[15,16] Melanoma cells can be more resistant to apoptosis than other cancer cells.[17]

The use of natural products in cancer therapy showed that plants are a most important source of antitumor compounds, with new structures and mechanisms of action being discovered.[18] Several plant-derived products induce apoptosis in neoplastic cells but not in normal cells.[19-23] Brazil has a vast territory with great plant diversity, since early times plants have been used to treat a large number of diseases including cancer. Many compounds with biological activity are obtained from Cerrado, Brazil's second largest bioma.[24] Several plant species from Cerrado are popularly used as herbal medicines for their reputed analgesic, anti-acid, antimicrobial, anti-inflammatory and anti-tumor properties.[25] The Experimental Oncology Unit routinely tests natural products for anti tumor activities mainly focusing on melanoma. *Pyrostegia venusta* (Ker Gawl.) Miers (Bignoneaceae), a native plant from the Brazilian Cerrado, was selected by surveying different species from this biome based on their cytotoxic and antitumor potential in the experimental B16F10 melanoma model.

P.venusta is popularly known as St. John vine or flame vine.[26] This ornamental species exhibits medicinal properties. Its flowers are used in popular medicine for treating leucoderma, diarrhea, cough and diseases of the respiratory system such as bronchitis, influenza and common cold.[27,28] In the present work we studied the cytotoxic effect of different extracts from *P.venusta* flowers. The crude extract showed a cytotoxic potential against melanoma cells with evidence of tumor cell apoptosis. Bioguided fractionation of a heptane extract (HE) that showed anti-tumor activity rather than a number of aqueous extracts yielded an active fraction (HEF2), which was cytotoxic in murine melanoma B16F10-Nex2 cells *in vitro* and in a syngeneic system *in vivo*. Analysis of active fraction using ^{1}H NMR as well as GC-MS indicated the presence of a mixture of straight chain saturated aliphatic hydrocarbons, with octacosane ($C_{28}H_{58}$) and triacontane ($C_{30}H_{62}$) as the predominant species. Individually, octacosane and triacontane were evaluated for their antitumor potential *in vitro* and *in vivo* and showed high cytotoxicity against murine melanoma B16F10-Nex2 cells besides inducing protection against a grafted subcutaneous melanoma. Both alkanes display a great potential as antitumor agents for topical use when the size and distribution of the tumor makes surgery a difficult procedure, as in many cases of acral lentiginous melanoma.

MATERIAL AND METHODS

Ethics statement

All necessary permits were obtained for the described field studies, granted by the State of São Paulo Research Support Foundation (FAPESP), Brazil, and the Brazilian National Research Council (CNPq) for collection of plant material in a privately owned ground by University of São Paulo, Assis-SP, Brazil. The procedures involving plant material were applied in accordance with label guideline and the field studies did not involve endangered or protected species. Tumor cell lines were originally obtained from the Ludwig Institute for Cancer Research, São Paulo, Brazil, being certified for research use. These are long established cell lines, acquired from public culture collections or transferred to the Ludwig Institute and maintained in appropriate conditions to serve as standard tumor cell lines for local studies and collaborative research. Animal experiments

were carried out using protocols approved by the Ethics Committee for Animal Experimentation of Federal University of São Paulo, Brazil and the specific Project presented by the Experimental Oncology Unit, including the animal experiments herein reported, has been approved via doc by Ethics and Research Committee (CEP) under the number 1234/2011.

Plant material and extraction procedure

Flowers of Pyrostegia venusta (Miers) (Bignoniaceae) were collected at Patos de Minas county, Minas-MG (18º31'40.34"S e 46º32'19.75"W). The plant material was identified by MSc. Alice de Fátima Amaral and a voucher specimen was deposited in the Mandevilla Herbarium at the Centro Universitario de Patos de Minas (UNIPAM) under the number MGHM0430. The hydroalcoholic extract (HA) was obtained from 50g of powdered flowers macerated in 250mL of EtOH: H_2O 7:3 (v/v) for 3 h at 60°C. Chloroform (CE) or heptane (HE) extracts were obtained from 20g of powdered flowers extracted three times with 200mL of heptane or chloroform with stirring for 2 h at room temperature. The extracts were filtered, dried under pressurized nitrogen and stored at-20°C. The dry extracts were reconstituted with 100% (v/v) dimethylsulfoxide (DMSO) to prepare a stock solution at a concentration of 10 mg/ml., Bioguided fractionation of crude heptane extract (HE).

Part of a crude heptane extract (HE) from flowers of *P. venusta* (600mg) was subjected to silica gel column chromatography eluted with hexane containing increasing amounts of ethyl acetate (up to 100%), to give 54 samples that were pooled into five fractions (HEF1-HEF7) after Thin Layer Chromatography (TLC) analysis. The different fractions were tested for cytotoxicity using a murine melanoma (B16F10-Nex2) growth inhibition test. The cytotoxic potential of the heptane extract was detected only in the fraction pool HEF2 (12mg), therefore this was analyzed by ^{1}H NMR spectroscopy as well as GC-MS aiming at the identification of active compounds. The most abundant compounds found in HEF2, octacosane and triacontane were evaluated for their cytotoxic activity on tumor cells and were purchased from Santa Cruz Biotechnology, Inc (California, USA). Alkanes were diluted in Roswell Park Memorial Institute medium (RPMI-1640) with 0.1% n-hexane and 1% DMSO, vortexed and sonicated for 5 min for further incubation with 1×10^4 B16F10-Nex2 cells. Negative controls were performed with vehicle (0.1% n-hexane and 1% DMSO in RPMI-1640).

Nuclear magnetic resonance and GC-MS analysis

Silica gel (Merck 230-400 mesh) was used for column chromatography and silica gel 60 PF_{254} (Merck) for analytical (0.25mm) TLC. Nuclear Magnetic Resonance (NMR) spectra were recorded at 200 MHz for ^{1}H nucleus on a Bruker AC200 spectrometer, using $CDCl_3$ as solvent and TMS (tetramethylsilane) as internal standard. GC-MS analysis was performed at 70 eV in an INCOS 50 Finnigan-Mat-quadrupole spectrometer, using a capillary column (DB-5) coated with crosslinked methyl silicone gum (50m, 0.20mm i.d., film thickness 0.33μm). The temperature program was 100°C isothermal for 1 min, then 100–280°C at 10°C/min, and isothermal at 280°C for 20 min. The temperature of injection and detection were 250 and 280°C, respectively.

Cell lines and culture

The following cell lines were used: human melanoma cell lines (SKMel 28 and A2058), originally provided by Dr. Alan N. Houghton of Memorial Sloan Kettering Cancer Center, NY; murine melanoma (B16F10-Nex2), a subclone of the B16F10 cell line obtained at the Experimental Oncology Unit (UNONEX), Federal University of São Paulo; human cervical cancer (HeLa), human umbilical vein endothelial cells (HUVEC), mouse fibroblasts (3T3) and human foreskin fibroblast (HF) cell lines were provided by Ludwig Institute for Cancer Research, São Paulo and Dr. Luiz F. Lima Reis, Hospital Sirio-Libanez, São Paulo, Brazil The U87-MG glioblastoma cell line was provided by Dr. Osvaldo K. Okamoto, University of São Paulo. Murine, syngeneic, colorectal adenocarcinoma cell (CT26) and murine pancreatic cells (PANC) were provided by Dr. Guillermo Mazzolini from the School of Medicine of Austral University, Derqui-Pilar, Buenos Aires, Argentina. Tumor cells were cultured at 37°C in a humidified atmosphere containing 5% CO_2, in RPMI 1640 medium (Invitrogen, Carlsbad, CA) supplemented with 10mM N-2-hydroxyethylpiperazine-N_2-ethanesulfonic acid (Hepes) (Sigma, St. Louis, MO), 24mM sodium bicarbonate (Sigma), 40mg/l gentamicin (Schering-Plough, São Paulo, Brazil), pH 7.2 and 10% fetal calf serum (Invitrogen). Human HF, mouse CT26 and 3T3 cells were maintained in DMEM supplemented as for the RPMI-1640 medium.

Cytotoxicity assay *in vitro*

P.venusta extracts and fractions were diluted in supplemented RPMI medium with 0.5% dimethyl sulfoxide (DMSO, SIGMA) and incubated with 5×10^3 or 1×10^4 murine and human tumor cells in 96-well plates. After a pre-incubation period (18 h), cell viability was assessed using the Cell Proliferation Kit I (MTT) (Boehringer Mannheim), a 3-(4,5-dimethylthiazol-2-yl)-2,5-diphenyltetrazolium bromide-based colorimetric assay. Readings were made in a plate reader at 570 nm. Alternatively, cell viability was accessed by the Trypan blue (Gibco, Grand Island, NY) exclusion test. All experiments were performed in triplicate.

Chromatin condensation analysis

B16F10-Nex2 cells (1×10^4) were cultivated on round coverslips, treated with 50 μg/ml of HE for 18 h, washed in PBS and fixed for 30 min at room temperature with 2% formaldehyde. The cells were washed in PBS and stained with 2μM Hoechst 33342 (Invitrogen) for 15 min and analyzed by fluorescence microscopy (Olympus BX-51 fluorescence microscope with immersion oil, at 60X magnification).

DNA fragmentation assay

DNA fragmentation of tumor cells was analyzed by the Terminal Deoxynucleotidyl Transferase dUTP Nick end Labeling (TUNEL) assay. 5×10^4 B16F10-Nex2 cells were incubated with 50μg/ml HE for 18 h and then processed and analyzed as previously described.[29] Combretastatin A4 (CA4) was used at 150 μM as positive controle of DNA fragmentation. Alternatively, DNA fragmentation was accessed by electrophoresis. 1×10^6 B16F10-Nex2 cells were incubated with 50μg/ml of HE at 37°C for 24 h and then genomic DNA were extracted from the cells, processed and analyzed as previously described.[30]

Annexin V and propidium iodide labeling

B16F10-Nex2 (3×10^5) cells were grown for 24 h in a 12-well plate and further incubated with 25 and 12μg/ml of HE or RPMI medium for 1 or 2 h at 37°C. The cells were harvested with cold PBS after three washes in the same buffer. Apoptotic cells were analyzed using the ApoScreen Annexin V-FITC kit according to the manufacturer's instructions (Southern Biotechnology, Birmingham, AL). Positive annexin V (AV) and propidium iodide cells were detected on an inverted fluorescence microscope (Olympus IX70) at 100X magnification.

Detection of caspase activity

The activity of caspases induced by HE was assessed using the *ApoTarget*™ Caspase Colorimetric Protease Assay Kit (Invitrogen, Carlsbad, CA) according to the manufacturer's protocol. 1×10^7 B16F10-Nex2 cells were seeded in 6-well plates and treated with 50 μg/ml of HE for 18 h. Briefly, cells were harvested and lysed in a lysis buffer for 10 min in ice. The lysate was centrifuged at 10,000*g* for 1 min, and 200 μg protein was incubated with 50 μl of the reaction buffer and 5 μl of the substrate, at 37°C for 2 h. The absorbance of the reaction mixture was quantified at 405 nm in a microplate reader (Spectramax M3, Molecular Devices).

N-acetylcysteine assay

B16F10-Nex2 cells (1×10^4) were seeded in 96-well plates for 6 h, pre-incubated with 10mM of N-acetylcysteine (NAC) for 2 h, washed twice in PBS and incubated with 50 μg/ml of HE for 18h at 37°C. In the control group, tumor cells were pre-incubated with RPMI. Cell viability was determined by Trypan blue (Gibco, Grand Island, NY) exclusion test.

Enhanced superoxide anion production

Enhanced superoxide anion production was detected by dihydroethidium (DHE) assay (Invitrogen) performed according to manufacturer's instructions. B16F10-Nex2 cells (5×10^4) were cultivated in 24-well plates and treated with 25 and 12 μg/ml of HE for 18 h. The cells were incubated with 5 μM DHE at 37°C for 30 min. For positive staining control, cells were treated with 5mM hydrogen peroxide for 30 min. Negative controls were treated with RPMI medium. The conversion of DHE to ethidium by oxidation was observed by fluorescence microscopy with an inverted fluorescence microscope (Olympus IX70) at 20X magnification.

Assessment of mitochondrial membrane potential (ΔΨm)

B16F10-Nex2 (1×10^5) cells were grown for 24 h in a 12-well plate and were incubated with 25 and 12 μg/ml HE at 37°C for 18 h. Cells were gently washed in PBS and loaded with 20nM of tetramethylrhodamine ethyl ester (TMRE, Molecular Probes, OR) for 10 min at 37°C. Cells were immediately observed with the aid of an inverted fluorescence microscope (Olympus I x 70) at 20X magnification.

Cell cycle analysis

B16F10-Nex2 (3×10^5) cells were incubated with 25 μg/ml of HE for 24 h. Cells were washed three times in PBS and pelleted at 1,500 rpm for 5 min. Cells were suspended and fixed in 2.5 ml ethanol (70% in PBS) for 15 min in ice. Cells were pelleted and suspended in 500 μl of PI solution in PBS (50 μg/ml propidium iodide, 0.1mg/ml RNase A and 0.05% Triton X-100) for 40 min at 4°C. Cells were pelleted and suspended in 500μl PBS for flow analysis on a Facs CantoII flow cytometer (BD Biosciences). Data were analyzed by Flowjo software (Tree Star, Inc. Ashland, OR).

Peritumor treatment of subcutaneously grafted murine melanoma

Six-week-old male C57BL/6 mice obtained from the Center for Development of Experimental Models (CEDEME), Federal University of São Paulo (UNIFESP) (average weight of 25-28g), were subcutaneously injected with 5×10^4 B16F10-Nex2 tumor cells. Peritumor injections were given starting 24 h after tumor cell graft. Treated groups (5 animals per group) received daily doses of 400μg of HE or 500μg of alkanes and the control groups received 5% DMSO in PBS (HE control) or 0.1% hexane, 5% DMSO in PBS (alkanes control). The use of 5% DMSO as vehicle was based on previous *in vivo* protocols

described in the literature.[31-33] Tumor size was measured daily for two weeks with a caliper, using the formula $V = 0.52 \times D1^2 \times D2$, where D1 and D2 are the short and long tumor diameters respectively, until the tumor volume reached a maximum of 3000mm^3, when the animals were sacrificed. The guidelines of the Animal Ethics Committee of Federal University of São Paulo (UNIFESP) were used for animal manipulation and experimental protocols (CEP 1234/2011).

Statistical analysis

All *in vitro* experiments were performed in triplicates. Student's *t* test was used for statistical analysis of *in vitro* and *in vivo* experiments. The IC_{50} value and 95% confidence intervals were calculated using GraphPad Prism 5 (GraphPad Software Inc., San Diego, CA) and Instat Plus 3 (The University of Reading, United Kingdom). Gehan-Breslow-Wilcoxon Test was used for the *in vivo* statistics.

RESULTS

Cytotoxic effect of *P.venusta* extracts on murine melanoma cells

The *P.venusta* flower hydroalcoholic extract (HA) showed low cytotoxic effect on B16F10-Nex2 cells as indicated by IC_{50} values higher than 100 μg/ml [Table 1]. Hydrophobic extracts, either in chloroform (CE) or heptane (HE) were also evaluated, and the HE extract showed the strongest cytotoxic activity in B16F10-Nex2 cells, with IC_{50} value of 28.96 μg/ml, compared to CE with IC_{50} of 70.93 μg/ml [Table 1]. Positive control was carried out with doxorubicin [Table 1], a well known antitumor compound.[34] Nontumor cells 3T3, HF and Huvec were less affected by HE extract than B16F10-Nex2 cells [Figure 1].

Evidence of apoptosis

Morphological changes on B16F10-Nex2 cells were observed after cell incubation with 50 μg/ml of HE for 18 h. Cellular blebs, likely apoptotic bodies and shrinkage of the cytoplasm were seen [Figure 2a]. Analysis of the genomic integrity, chromatin condensation and DNA fragmentation, was also examined as indicators of apoptosis.[7] Chromatin condensation was visualized in 30% of 1×10^4 B16F10-Nex2 cells treated with 50 μg/ml HE for 18 h and stained with Hoechst 33342 [Figure 2b].

Cleavage of chromosomal DNA into oligonucleosomal fragments was evaluated by electrophoresis gel of the tumor cell DNA extract after cell incubation with 50 μg/ml of HE for 24 h, and ladder fragmentation pattern was observed [Figure 2c]. Alternatively, the DNA fragmentation was assessed using TUNEL staining, resulting in 74% of TUNEL positive cells (green), compared to the negative control, which showed no TUNEL positive cells [Figure 2d].

Exposure of phosphatidylserine on the cell surface during apoptosis was also shown in HE treated cells as measured by the increased binding of Annexin V. After 18 h of cell incubation with 25 μg/ml of HE, 45% of the cells were at early apoptosis stage (Annexin $^+PI^-$) and 6% were at late apoptosis (Annexin $^+PI^+$), compared to the negative control. No primary necrosis (Annexin$^-PI^+$) was detected in treated cells [Figure 3a].

Treatment of B16F10-Nex2 cells with HE also rendered a significant increase in the activation of caspases 2, 3, 8 and 9 [Figure 3b], clearly defining the apoptotic response.

Enhanced superoxide anion production

Enhanced superoxide anion production in B16F10-Nex2 cells was observed after treatment with 12 and 25 μg/ml of HE for 18 h [Figure 4a]. About 60% of tumor cells treated with 25 μg/ml of HE showed enhanced superoxide anion production detected by dihydroethidium (DHE). In comparison, positive control cells incubated with 5mM of hydrogen peroxide for 30 min showed 65% DHE positive cells [Figure 4c]. Pre-incubation of B16F10-Nex2 cells with *N*-acetyl-L-cysteine (NAC) followed by incubation with HE increased cell viability by 30% ($P = 0.013$) compared to NAC-untreated cells [Figure 4d].

Table 1: IC_{50} values of *P. venusta* extracts on B16F10-Nex2 cells *in vitro*

P.venusta extract	IC_{50} (μg/ml)	SD (μg/ml)
HA (hydroalcoholic extract)	>100	-
CE (Chloroform extract)	70.93	±1.34
HE (heptane extract)	22.5	±1.08
[a]Doxorrubicin	1.4	±0.30

[a]Positive control

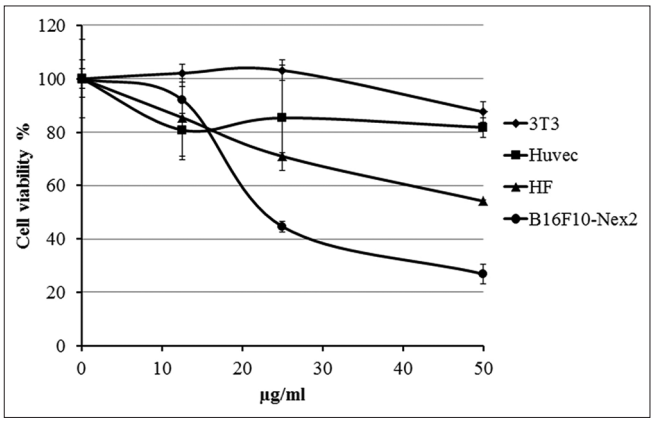

Figure 1: Cytotoxicity of HE in B16F10-Nex2 murine melanoma and nontumorigenic HUVEC, HF and 3T3 cells. Dose dependent activity of HE over 104 tumor cells in 18 h

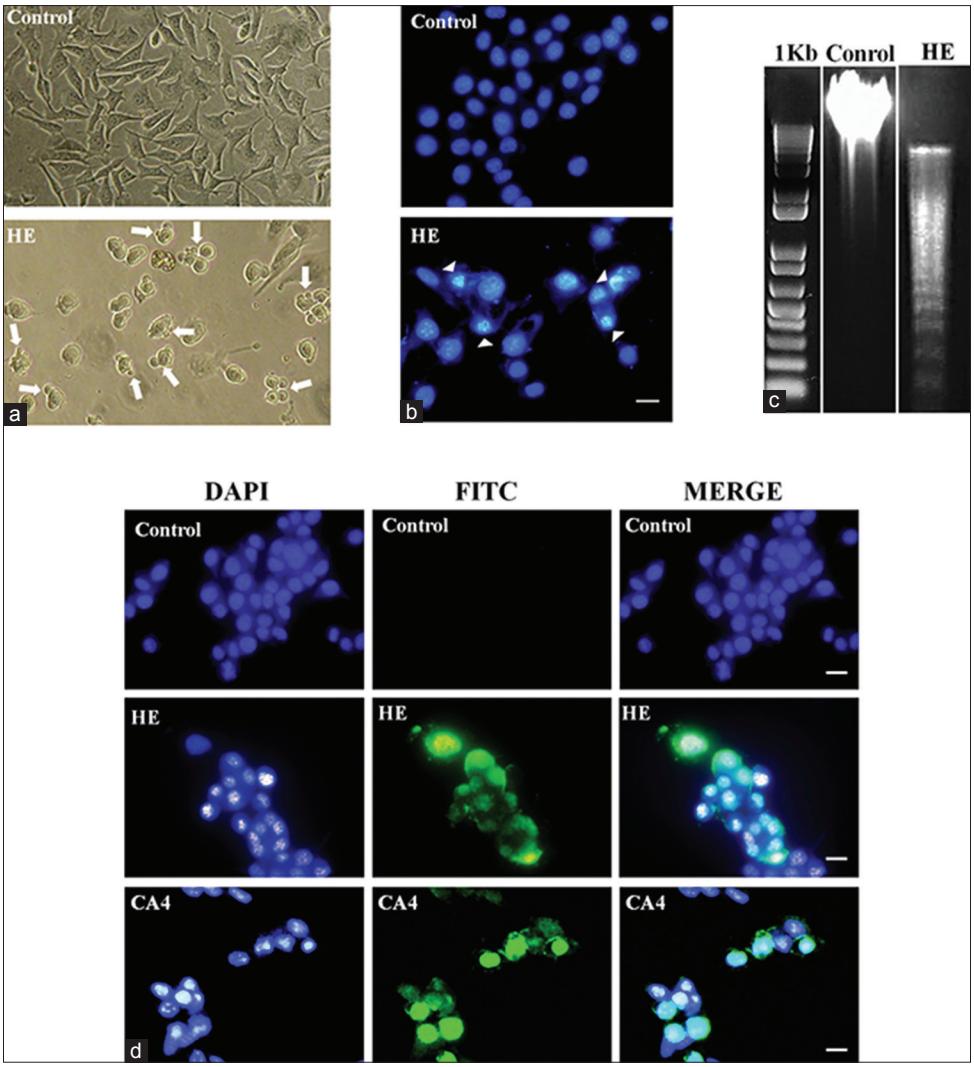

Figure 2 : Morphological evidence and DNA degradation in HE-treated apoptotic melanoma cells. (a) B16F10-Nex2 cell morphology after treatment with 50 µg/ml HE for 18 h. Apoptotic bodies' formation is indicated by white arrows; (b) Evaluation of chromatin condensation in HE treated cells. B16F10-Nex2 cells (104) were treated with 50µg/ml of HE for 18 h, labeled with Hoechst dye, and analyzed by fluorescence microscopy. Arrows indicate pronounced chromatin condensation in treated cells (Magnification 60x) Scale bar: 20µm; (c) Agarose gel electrophoresis of DNA fragmentation in B16F10-Nex2 cells induced by 50 µg/ml HE treatment for 24 h; (d) Fluorescence microscopy for DNA fragmentation. Melanoma cells (5 × 104) were treated with 50 µg/ml of HE and 150 µM of combretastatin A4 as positive apoptotic control for 24 h, and DNA fragmentation was detected using a TUNEL assay (green fluorescence). DAPI (blue) were used for total cell nuclei (Scale bar: 20 µm)

Inner mitochondrial membrane potential

B16F10-Nex2 cells were incubated with TMRE, a fluorescent probe used to measure $\Delta\Psi m$ in mitochondria. In resting conditions, mitochondria appeared as elongated structures regularly distributed in the cell cytoplasm. HE-treated cells showed a significant breakdown of the mitochondrial membrane potential measured by the decrease in 91.6 and 60% of TMRE fluorescence in cells treated with 25 µg/ml and 12 µg/ml HE, respectively, compared to untreated control cells [Figure 4b and c].

HE induces G2/M cell cycle arrest in tumor cells

Treatment of tumor cells with 25 µg/ml of HE for 18 h increased the percentage of cells in G2/M phase with a significant reduction of the S phase [Figure 5a]. Positive control was carried out with CA4. The cell cycle arrest induced by HE was accompanied by morphological changes in the cell volume [Figure 5b].

In vivo antitumor activity of HE

The antitumor protective effect of HE was evaluated in C57Bl/6 mice challenged subcutaneously with 5×10^4 B16F10-Nex2 cells. Daily doses of 400 µg of HE were injected in 100 µl of vehicle (5% DMSO in PBS) at peripheral sites to the original cell grafting. Treatment resulted in a significant decrease in tumor volume as seen from the 14th day of treatment with a potent antitumor effect of HE compared to the vehicle treated

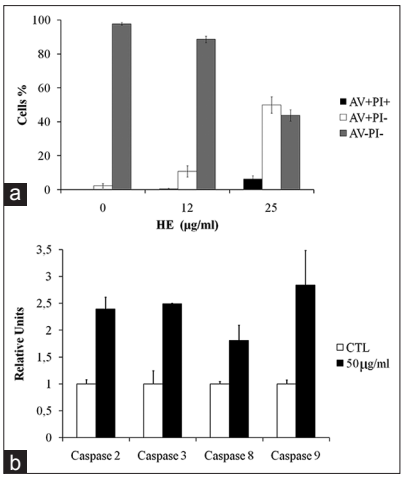

Figure 3: Phosphatidyl serine surface expression and caspase activation. (a) Annexin V and propidium iodide labeling of B16F10-Nex2 (3 x 105) cells grown for 24 h in 12-well plate and incubated with 12 and 25 µg/ml of HE or RPMI medium for 18 h at 37 °C. Positive annexin V (AV) and propidium iodide cells were detected with an inverted fluorescence microscope at 10X magnification; (b) Activation of caspase-2, 3, 8 and 9 in HE treated melanoma cells. B16F10-Nex2 cells (107) were treated with 50 µg/ml of HE for 24 h, and the HE induced enzymatic activity of caspase-2, 3, 8 and 9 was evaluated by colorimetric assay

control [Figure 6]. In addition, no toxic effects, loss of weight, or alteration in animal behavior were observed during the treatment with HE.

Bioguided fractionation of HE extract and chemical analysis

The crude HE extract was subjected to a bioguided fractionation procedure, in which seven pooled fractions (HEF1, HEF2, HEF3, HEF4, HEF5, HEF6 and HEF7) were evaluated for their cytotoxic activity on murine melanoma cells *in vitro*. The cytotoxic acitivity on B16F10-Nex2 cells was restricted to pooled fraction HEF2 with IC_{50} of 28.48 µg/ml [Figure 7]. Cytotoxicity of HEF2 was also observed against several other tumor cell lines, as shown in Table 2.

The ^1H NMR spectrum of HEF2 (in $CDCl_3$) depicted an intense singlet at δ 1.18 ppm, a multiplet at δ 1.51 ppm and a deformed triplet at δ 0.81 ppm (J = 6.8 Hz) [Figure 8a]. These signals, associated to the absence of signals at range of δ 5-6 ppm, characteristic of hydrogens linked at unsaturated sp^2 carbons, suggested the predominance of long side chain saturated hydrocarbons.[35,36] Analysis by GC-MS indicated that this fraction was composed by thirteen compounds [Table 3], which were identified as a mixture of hydrocarbons (71.18%): tetracosane ($C_{24}H_{50}$-6.92%), hexacosane ($C_{26}H_{54}$-7.23%), heptacosane ($C_{27}H_{56}$-2.72%), octacosane ($C_{28}H_{58}$-36.34%), nonacosane ($C_{29}H_{60}$-2.70%), triacontane ($C_{30}H_{62}$-12.72%), and dotriacontane ($C_{32}H_{66}$-2.55%) as well as by oxygenated derivatives in minor

Table 2: IC_{50} values of HEF2on different tumor cell lines *in vitro*

Cell lineage	IC_{50} (µg/ml)	SD (µg/ml)
A2058	62.04	±1.66
U87	48.60	±1.18
SIHA	38.48	±1.57
HCT	16.01	±0.63
SKmel28	10.76	±0.50
CT26	33.84	±0.35
B16F10-Ne×2	28.48	±1.02
4T1	13.32	±0.23
PANC	8.36	±0.84

PANC: Pancreatic cells; HEF: Heptane extract fraction

Table 3: Identification of saturated hydrocarbon derivatives and other compounds in group HEF2 from heptane extract from flowers of *Pyrostegia venusta*

Molecular formula	Identified compound	Relative amount/%
$C_6H_{12}O$	3-methyl-2-pentanone	1.13
$C_6H_{14}O$	3-methyl-3-pentanol	3.54
$C_6H_{14}O$	3-hexenol	0.83
$C_6H_{14}O$	4-methyl-2-pentanol	0.65
$C_5H_8O_2$	Allyl acetate	1.65
$C_7H_{14}O$	2,2-dimethylpentanal	4.79
$C_{24}H_{50}$	Tetracosane	6.92
$C_{26}H_{54}$	Hexacosane	7.23
$C_{27}H_{56}$	Heptacosane	2.72
$C_{28}H_{58}$	Octacosane	36.34
$C_{29}H_{60}$	Nonacosane	2.70
$C_{30}H_{62}$	Triacontane	12.72
$C_{32}H_{66}$	Dotriacontane	2.55

HEF: Heptane extract fraction

proportion (12.59%): 3-methyl-2-pentanone (1.13%), 3-methyl-3-pentanol (3.54%), 3-hexenol (0.83%), 4-methyl-2-pentanol (0.65%), allyl acetate (1.65%), 2,2-dimethylpentanal (4.79%). The characterization of these compounds was based on the comparison of recorded mass spectra with those available in the database as well as their retention times in a DB-5 column [Figure 8b], after co-injection of standards, as represented for octacosane [Figure 8c] and triacontane [Figure 8e].

In vitro cytotoxic activity of Octacosane and Triacontane

Since octacosane and triacontane were found in higher amounts in the HEF2 fraction, they were evaluated for cytotoxic activity on B16F10-Nex2 melanoma cells. Octacosane and triacontane were purchased from Santa Cruz Biotechnology, Inc (California, USA). Alkanes were incubated with 1 × 10^4 B16F10-Nex2 cells at different

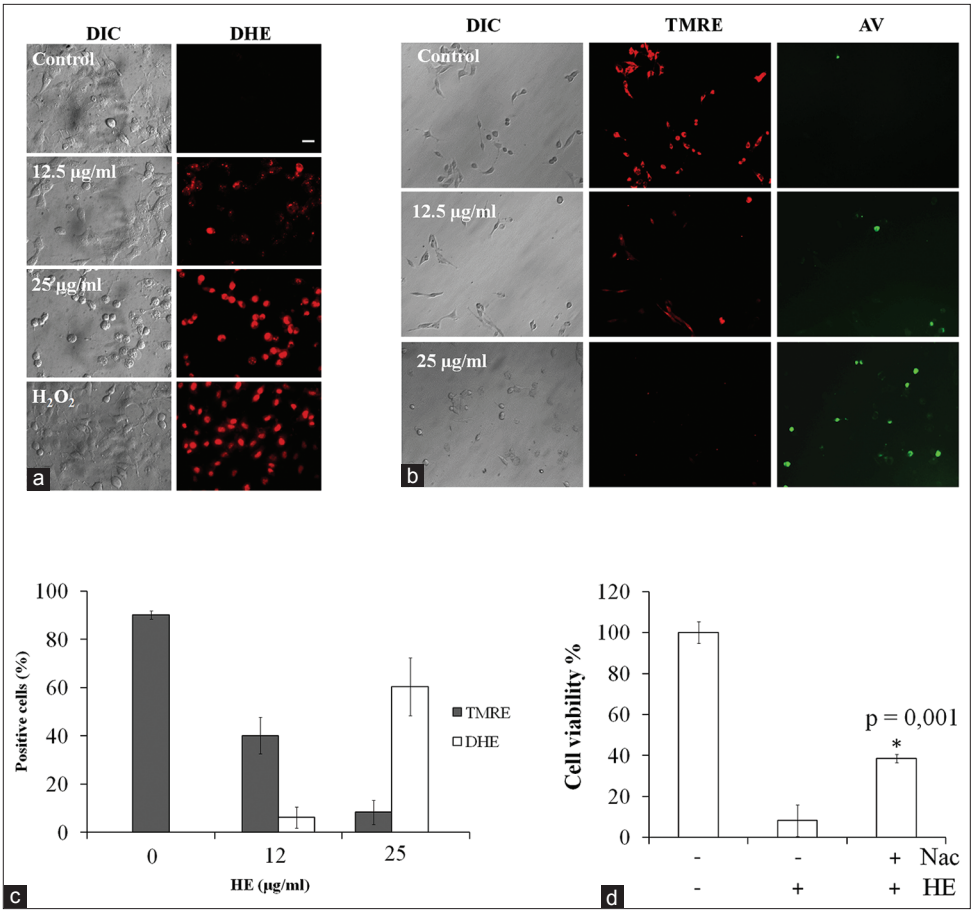

Figure 4: Mitochondrial effects of HE treatment. (a) Representative images of superoxide anions' negative and positive cells treated with 12.5 and 25 µg/ml of HE for 18 h, and 5 mm of hydrogen peroxide (positive control) for 30 min. B16F10-Nex2 cells were stained with 5 µM of DHE (dihydroethidium). Scale bar: 20 µm; (b) Representative images of mitochondrial ΔΨm following HE treatment. B16F10-Nex2 cells were treated with negative control and with 12 and 25 µg/ml of HE for 18 h (original magnification, 20×). Positive apoptotic cells were stained with annexin V (original magnification, 10X). (c) Percentage of TMRE (tetramethylrhodamine ethyl ester) and DHE positive cells; (d) Protective effect of N-acetyl cysteine (NAC) on HE-treated cells. B16F10-Nex2 cells (104) were pretreated for 2 h with 10 mM NAC, washed and incubated with 50 µg/ml of HE at 37°C for 18 h

concentrations and we observed that both alkanes displayed strong cytotoxic activity on B16F10-Nex2 cells, with IC_{50} values of 20.9 µg/ml and 41.08 µg/ml for triacontane and octacosane, respectively [Figure 9a]. We also observed that both alkanes induced similar morphological changes as those induced by HE treatment in B16F10-Nex2 cells [Figure 9b].

In vivo antitumor activity of Octacosane and Triacontane

The antitumor activities of octacosane and triacontane were investigated in subcutaneous melanoma model. 5×10^4 B16F10-Nex2 Cells were injected subcutaneously in C57Bl/6 mice and daily doses of 500 µg of Octacosane and Triacontane were injected at peripheral sites in relation to the original cell grafting. Treatment procedure resulted in a significant delay of tumor progression with a significant antitumor effect of octacosane ($P = 0.017$) and triacontane ($P = 0.04$) compared to the vehicle control (5% DMSO in PBS) [Figure 6]. In addition, the survival rate of treated groups was significantly increased in triacontane ($P = 0.018$) and octacosane ($P = 0.032$) treated animals [Figure 10b]. No toxic effects, loss of weight, or alteration in animal behavior were observed during the treatment with octacosane and triacontane.

DISCUSSION

In this study, we observed that fractions and compounds in the heptanic extract of flowers from *Pyrostegia venusta* exhibit promising cytotoxic activity against malignant melanoma *in vitro* and *in vivo*, which enhances the therapeutic opportunities that this plant fits to be used in the treatment of different diseases.[37]

We show that murine melanoma cells react to the heptane extract of *P. venusta* by undergoing apoptosis. Hallmarks of apoptosis such as plasma membrane blebbing without

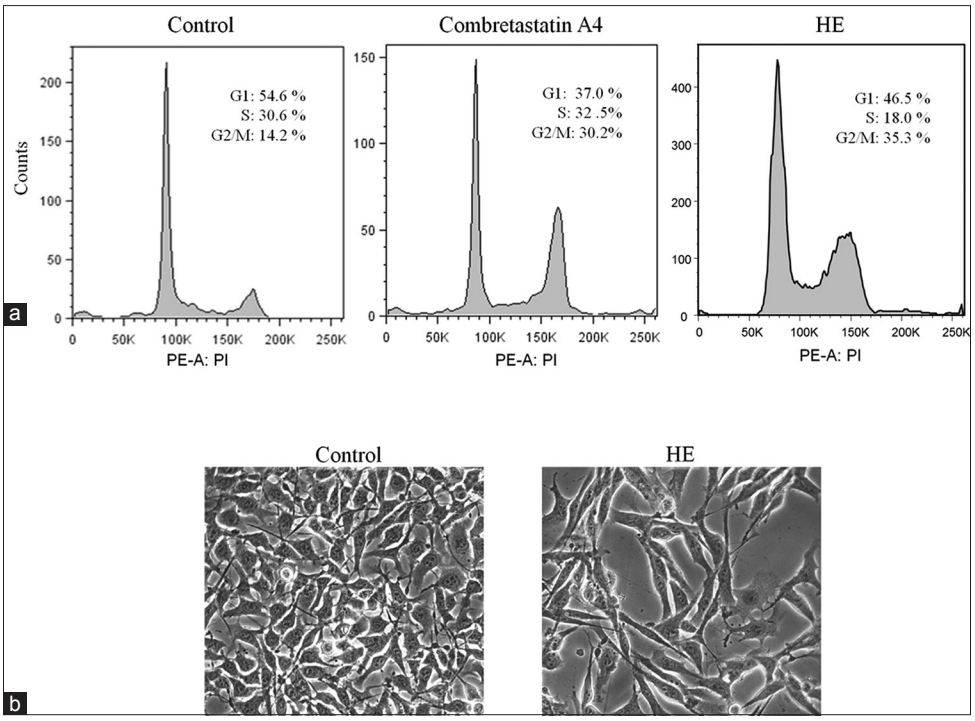

Figure 5: Effect of HE on the melanoma cell cycle. (a) Cell cycle analysis of B16F10-Nex2 tumor cells treated with 25 µg/ml HE and 75 µM of CA4 for 24 h. (b) Representative images of tumor cell morphology following HE treatment

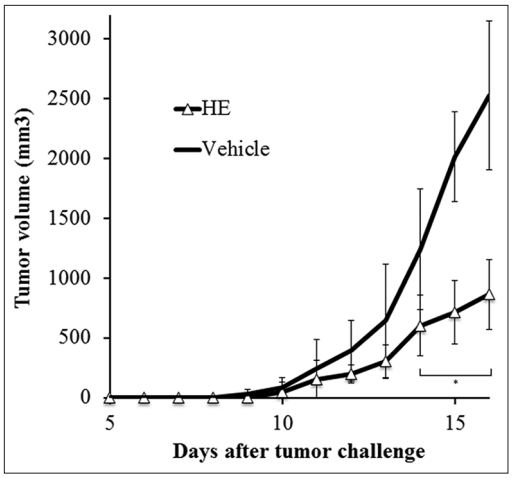

Figure 6: HE antitumor effect against subcutaneous melanoma. Six-week-old male C57BL/6 mice were injected subcutaneously with 5x104 B16F10-Nex2 tumor cells. Peritumor treatment started 24 h after tumor inoculation. HE (400 µg) in 100µl PBS was injected in daily doses and the tumor size was measured seven times a week with a caliper until the tumor volume reached a maximum of 3000 mm3, when animals were sacrificed. The control group was treated with PBS/DMSO 5%. **P*<0.05

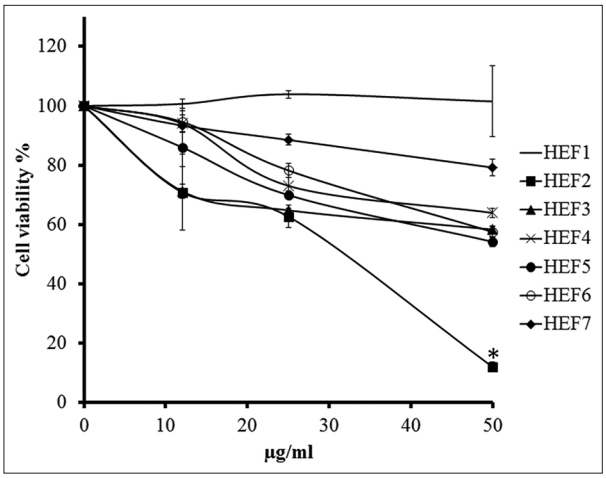

Figure 7: Tumor cell viability after treatment with HE fractions. B16F10-Nex2 cells (104) were seeded in 96-well plates and incubated with different concentrations of HE fractions for 24 h. Assays were performed in triplicates. **P*<0.05

lysis, cell shrinkage, mitochondria permeabilization, chromatin condensation and DNA fragmentation, and phosphatidylserine surface expression were observed during the treatment of murine melanoma cells with HE *in vitro*, confirming the apoptotic nature of cell death.[7,38]

Apoptosis can be variously induced, as by death receptor ligands interacting on the plasma membrane (receptor or extrinsic pathway) or by mitochondrial pathways (intrinsic pathway).[39] We suggest that the mechanism by which HE treated cells undergo apoptosis is related to the intrinsic pathway, as evidenced by the production of superoxide anions in the mitochondria of HE treated cells. Free radicals, particularly ROS, have been proposed as common mediators of apoptosis.[38,40] Mitochondria are involved in the production of reactive oxygen species, mainly superoxides and hydrogen peroxide and mitochondrial membrane damage results in the leakage of superoxide anions into the cytosol.[41]

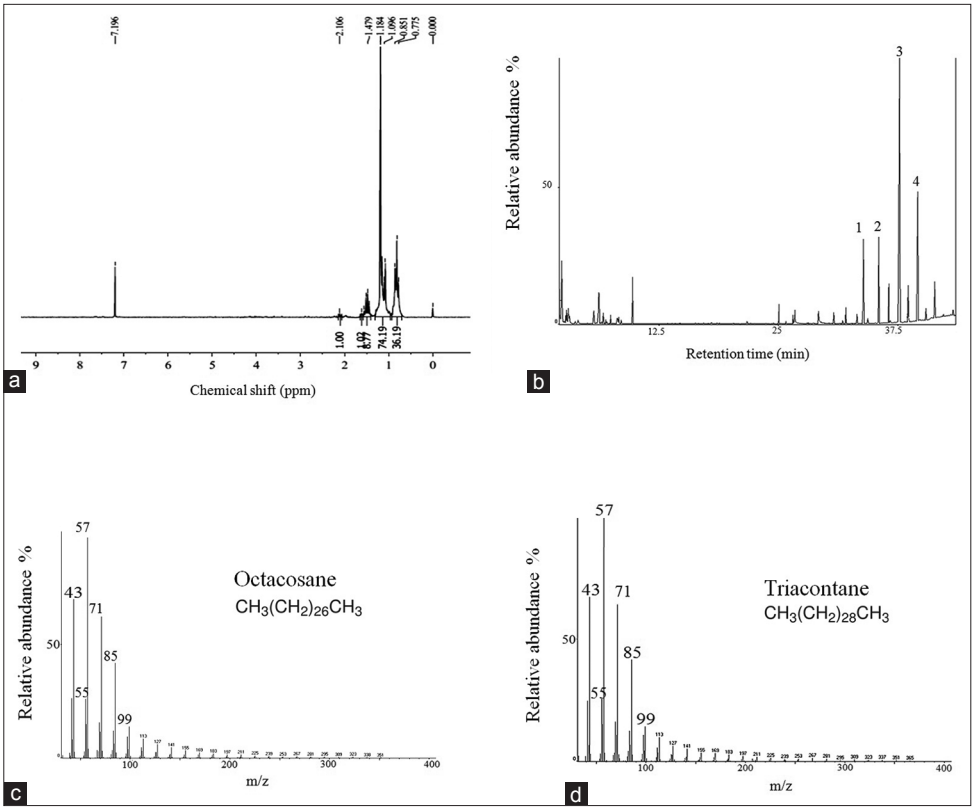

Figure 8: (a) 1H NMR spectrum of fraction HEF2 (~ CDCl3, 200 MHz)-the signal at ~ 7.24 ppm corresponding to hydrogens of residual CHCl3 in deuterated solvent; (b) GC-MS of HEF2 components with 4 main alkane species with the retention times of (1) tetracosane (C24H50), (2) hexacosane (C26H54), (3) octacosane (C28H58), (4) triacontane (C30H62), and 3 other minor species as listed in Table 3; (c) Mass spectrum of octacosane (GC component 3) and (d) triacontane (GC component 4), further identified by co-injection with standard n-octacosane, Rt 37.7 min, MM 620 Da, and triacontane, Rt 39.57 min, MM 422 Da

In eukaryotic cells, plant derived compounds can promote dissipation of the mitochondrial membrane potential ($\Delta\Psi m$) resulting in leakage of pro-apoptotic factors mainly cytochrome c.[30] Once in the cytoplasm, cytochrome c associates with Apaf-1 and then procaspase-9 (and possibly other proteins) to form the apoptosome. Heat-shock proteins play a role in the pathway to modulate apoptosis. Caspase-9 activates other downstream caspases such as caspase-3 that constitute the major caspase activity in apoptotic cells.[42,43]

In a study with pyrimethamine in metastatic melanoma, this drug, which generates ROS, induced upstream caspase activation (caspase-8), bypassing CD95/Fas engagement.[44] Kim and colleagues also showed that N, N-dimethyl phytosphingosine could induce caspase-8-dependent cytochrome c release and apoptosis through ROS generation in human leukemia cells.[45] We observed that an apoptotic peptide (C7H2) inducing caspase 8 produced abundant superoxide anions in B16F10-Nex2 cells.[29] Other mechanisms by which ROS promote caspase-9 activation[46] have also been described. Oxidative modification of caspase-9 by ROS could mediate its interaction with Apaf-1, independently from the increased release of cytochrome c, and thus promote auto-cleavage and activation. Such mechanism may facilitate apoptosome formation and caspase-9 activation under oxidative stress conditions.[39]

We showed that HE treatment induced caspases 2, 3, 8 and 9, besides disruption of the mitochondrial membrane potential and release of superoxide anions. Caspase-2 activation could induce cell cycle regulation and tumor suppression.[47] It is unique among the caspases because it has features of both initiator and effector caspases.[48] Prasad and colleagues reported that ROS generation induce the activation of caspase-2 in human leukemic cells and the simultaneous activation of caspases 8 and 9. Cross-talk between these initiator caspases is mediated by the proapoptotic protein Bid.[49] It is possible that the HE induced activation of caspase-8 as mediated by ROS, and leading to apoptosis may involve the caspase-8-Bid-Bax pathway.

The antitumor activity of HE also involved the cell cycle arrest in over 40% treated cells. It is still unclear whether checkpoint genes are involved that could mediate mitochondrial apoptotic signaling,[50] or the expression and translocation of Bax.[51] Thus, specific studies of induced

cell death signaling should be performed with the isolated active compounds from HE in order to better characterize their mechanism of action involved in the induction of cell cycle arrest and apoptosis.

The cytotoxic potential of the heptane extract (HE) of *P.venusta* flowers on murine melanoma B16F10-Nex2 cells is related to the alkane rich active fraction, which is also active against several human cancer cells lines *in vitro*. HE was studied according to the criterion of the American National Cancer Institute, which states that the IC_{50} limit to consider a crude extract requiring further purification is 30 μg/ml.[52] Previous phytochemical studies on *P. venusta* flower extracts from India identified stigmasterol, β-sitosterol, β-amyrin and oleanolic acid compounds.[52] Recently, a complete characterization of phytochemicals occurring in the methanolic extract of *P.venusta* showed predominantly, myoinositol, hexadecanoic acid, linoleic acid, oleic acid, stigmasteryl tosylate, diazoprogesterone, arabipyranose. Moreover, these methanolic extracts showed antioxidant activity *in vivo* and *in vitro*, verified by DPPH, ABTS and FRAP assays, although the compounds responsible for the antioxidant activity were not investigated.[53,54]

In the present work, the active fraction HEF2 of the heptane extract of *P.venusta* flowers did not contain triterpenoids and/or steroids but rather, a mixture of saturated hydrocarbons in which triacontane and octacosane predominated. Previous works have shown that straight-chain saturated hydrocarbons have antitumor activities in different systems. Takahashi *et al*., (1995) have found that hentriacontane, the main component in their bioactive fraction, showed the highest antitumor activity.[55] This same compound predominates in the epicuticular wax in leaves from *Kigelia pinnata*, and is responsible for the plant protection against UV radiation and for its antitumour potential.[56] The saturated hydrocarbon gentriacontan ($C_{31}H_{64}$), present in the chloroform extract of *Clinopodium vulgare*, was reported to inhibit the growth of Erlich ascites tumor in mice, and also possesses antitumor activity against CEM and K-562 human leukemia cell lines *in vitro*.[57] Gomez-Flores *et al*., found that the observed antitumor activity against lymphoma cells was due primarily to the presence of hentriacontane in the leaves of *C. vulgare*.[58] More recently, it has been described that intracellular eicosanoid metabolites regulate mitochondrial function and induce apoptosis.[59] Recently, both octacosane and triacontane were found in the same proportions in a lipid fraction from the ether extract of *Solanum elaeagnifolium* as promising antibacterial agents.[60] Thus, the alkane rich HEF2 fraction from *P. venusta* flowers is in line with these studies, being responsible for the observed tumor apoptosis effects of HE.

Most importantly, mice treated with HE showed a marked reduction in the subcutaneous tumor progression indicating an important activity of this plant extract against primary melanoma, and the same antitumor activity *in vivo* was further confirmed when mice were treated with isolated octacosane and triacontane.

In this work, octacosane and triacontane had to be solubilized in low amounts of dimethylsulfoxide (DMSO) to be tested, and probably their anti-tumor effect depends on the alkane-DMSO complex formed. It has been

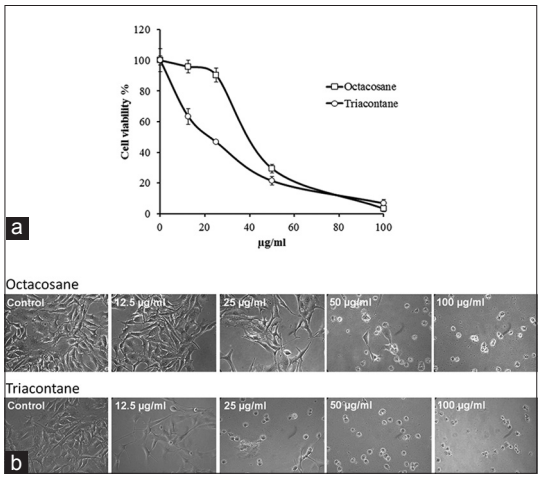

Figure 9: Cytotoxicity of HE individual alkanes. (a) Cytotoxicity of octacosane and triacontane in B16F10-Nex2 cells after 18 h. (b) Tumor cell morphology after incubation with different concentrations of octacosane and triacontane

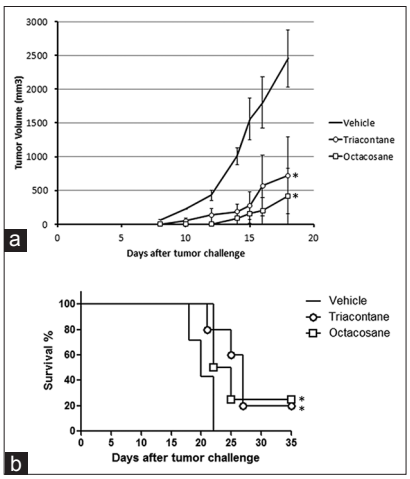

Figure 10: *In vivo* antitumor activity of Octacosane and Triacontane. Six-week-old male C57BL/6 mice were injected subcutaneously with 5×104 B16F10-Nex2 tumor cells. Peritumor treatment started 24 h after tumor inoculation. Five animals per group were used. Alkanes (500 μg) were injected in 100 μl of 5% DMSO in PBS. Daily doses were given during all treatment period. Tumor size was measured seven times a week with a caliper until the tumor volume reached a maximum of 3000mm^3 when the animals were sacrificed. The control group was treated with vehicle PBS/DMSO 5%. *P<0.05, indicates significant differences between groups

shown that in pure water, long chain n-alkane exhibits an intermittent oscillation between the collapsed and the extended coiled conformations. When the mole fraction of DMSO is 0.05, its concentration in the first hydration layer around the hydrocarbon of chain length 30 (n = 30) is of 17%. The formation of such hydrophobic environment around the hydrocarbon chain is the reason for the collapsed conformation gaining additional stability.[61] Such conformation of the alkane-DMSO combination allowed the observed antitumor activity of both octacosane and triacontane *in vitro* and *in vivo*, with no systemic toxicity observed in mice receiving DMSO alone.

Besides, DMSO presents great ability to penetrate tissues, which justifies its use in many therapeutical protocols in dermatology. It increases the effectiveness of the percutaneous penetration of many substances, facilitating their diffusion across the stratum corneum and promotes transport into the local blood vessels, as demonstrated by increasing the penetration of many agents, including 5-fluorouracil in the treatment of superficial tumors and warts.[62-65] Combination therapy of DMSO with different drugs enhances the healing of cutaneous diseases, such as acral lick dermatitis, arthritis, mastitis and scleroderma, and it is considered to have a low toxicity.[66,67] The current use of DMSO regards its application in intravenous, subcutaneous and oral routes. Several recent works have presented DMSO as vehicle of different anticancer compounds administered systemically or topically in 1 ~ 10% solution.[68-71]

CONCLUSION

The Experimental Oncology Unit routinely tests natural products for anti tumor activities mainly focusing on melanoma. As pointed out before (Introduction) several plant-derived products induce apoptosis in neoplastic cells but not in normal cells. The nature of the anti tumor agents varies in terms of distribution, solubility and chemical composition. Surprisingly, heptane extracts but not aqueous extracts of Pyrostegia venusta were cytotoxic to melanoma cells *in vitro* and *in vivo*, and the active compounds are saturated aliphatic hydrocarbons. Since peritumor injections of the active alkanes protected against melanoma in a mouse model, suggestion has been made that these compounds might also be therapeutic in mostly epidermal and slowly invasive human melanomas, such as acral lentiginous melanoma, as an adjuvant treatment to surgical excision. Regional perfusion chemotherapy in addition to excision is significantly more efficient in the treatment of acral melanoma than excision alone.

ACKNOWLEDGMENTS

The present work was supported by Fundação de Amparo à Pesquisa do Estado de São Paulo (FAPESP), and Conselho Nacional de Desenvolvimento Científico e Tecnológico (CNPq).

REFERENCES

1. Guimaraes FS, Abud AP, Oliveira SM, Oliveira CC, Cesar B, Andrade LF, *et al*. Stimulation of lymphocyte anti-melanoma activity by co-cultured macrophages activated by complex homeopathic medication. BMC Cancer 2009;9:293.
2. Sawada N, Kataoka K, Kondo K, Arimochi H, Fujino H, Takahashi Y, *et al*. Betulinic acid augments the inhibitory effects of vincristine on growth and lung metastasis of B16F10 melanoma cells in mice. Br J Cancer 2004;90:1672-8.
3. Ozben T. Mechanisms and strategies to overcome multiple drug resistance in cancer. FEBS Lett 2006;580:2903-9.
4. Krementz ET, Feed RJ, Coleman WP 3rd, Sutherland CM, Carter RD, Campbell M. Acral lentiginous melanoma. A clinicopathologic entity. Ann Surg 1982;195:632-45.
5. Rashid OM, Schaum JC, Wolfe LG, Brinster NK, Neifeld JP. Prognostic variables and surgical management of foot melanoma: Review of a 25-year institutional experience. ISRN Dermatol 2011;2011:384729.
6. Fidler IJ, Nicholson GL. Tumor cell and host properties affecting the implantation and survival of blood-borne metastatic variants of B16 melanoma. Isr J Med Sci 1978;14:38-50.
7. Kroemer G, Galluzzi L, Vandenabeele P, Abrams J, Alnemri ES, Baehrecke EH, *et al*. Classification of cell death: Recommendations of the Nomenclature Committee on Cell Death 2009. Cell Death Differ 2009;16:3-11.
8. Adams JM, Cory S. Bcl-2-regulated apoptosis: Mechanism and therapeutic potential. Curr Opin Immunol 2007;19:488-96.
9. Zeisel SH. Antioxidants suppress apoptosis. J Nutr 2004;134:3179S-80.
10. Kass GE, Eriksson JE, Weis M, Orrenius S, Chow SC. Chromatin condensation during apoptosis requires ATP. Biochem J 1996;318 (Pt 3):749-52.
11. Golstein P, Kroemer G. Cell death by necrosis: Towards a molecular definition. Trends Biochem Sci 2007;32:37-43.
12. Baehrecke EH. Caspase activation finds fertile ground. Dev Cell 2003;4:608-9.
13. Hanahan D, Weinberg RA. Hallmarks of cancer: the next generation. Cell 2011;144:646-74.
14. Hanahan D, Weinberg RA. The hallmarks of cancer. Cell 2000;100:57-70.
15. Raff M. Cell suicide for beginners. Nature 1998;396:119-22.
16. Banjerdpongchai R, Kongtawelert P, Khantamat O, Srisomsap C, Chokchaichamnankit D, Subhasitanont P, *et al*. Mitochondrial and endoplasmic reticulum stress pathways cooperate in zearalenone-induced apoptosis of human leukemic cells. J Hematol Oncol 2010;3:50.
17. Kluza J, Lansiaux A, Wattez N, Hildebrand MP, Léonce S, Pierré A, *et al*. Induction of apoptosis in HL-60 leukemia and B16 melanoma cells by the acronycine derivative S23906-1. Biochem Pharmacol 2002;63:1443-52.
18. Mashele S, Fuku SL. Evaluation of the antimutagenic and mutagenic properties of asparagus laricinus. Med Technol SA 2011;25:33-36

20. Youn MJ, Kim JK, Park SY, Kim Y, Park C, Kim ES, *et al*. Potential anticancer properties of the water extract of Inonotus [corrected] obliquus by induction of apoptosis in melanoma B16-F10 cells. J Ethnopharmacol 2009;121:221-8.
21. Park HJ, Han ES, Park DK. The ethyl acetate extract of PGP (Phellinus linteus grown on Panax ginseng) suppresses B16F10 melanoma cell proliferation through inducing cellular differentiation and apoptosis. J Ethnopharmacol 2010;132:115-21.
22. Hu W, Zhang C, Fang Y, Lou C. Anticancer properties of 10-hydroxycamptothecin in a murine melanoma pulmonary metastasis model *in vitro* and in vivo. Toxicol *In vitro* 2011;25:513-20.
23. Tavakkol-Afshari J, Brook A, Mousavi SH. Study of cytotoxic and apoptogenic properties of saffron extract in human cancer cell lines. Food Chem Toxicol 2008;46:3443-7.
24. Mesquita ML, de Paula JE, Pessoa C, de Moraes MO, Costa-Lotufo LV, Grougnet R, *et al*. Cytotoxic activity of Brazilian Cerrado plants used in traditional medicine against cancer cell lines. J Ethnopharmacol 2009;123:439-45.
25. Napolitano DR, Mineo JR, de Souza MA, de Paula JE, Espindola LS, Espindola FS. Down-modulation of nitric oxide production in murine macrophages treated with crude plant extracts from the Brazilian Cerrado. J Ethnopharmacol 2005;99:37-41.
26. Veloso CC, Bitencourt AD, Cabral LD, Franqui LS, Dias DF, dos Santos MH, *et al*. Pyrostegia venusta attenuate the sickness behavior induced by lipopolysaccharide in mice. J Ethnopharmacol 2010;132:355-8.
27. Ferreira DT, Alvares PS, Houghton PJ, Braz R. Chemical constituents from roots of Pyrostegia venusta and considerations about its medicinal importance. Quimica Nova 2000;23:42-6.
28. Cardozo NP, Parreira MC, Alves PL, Bianco S. Foliar area estimate of two sugarcane-infesting weeds using leaf blade linear dimensions. Planta Daninha 2009;27:683-7.
29. Arruda DC, Santos LC, Melo FM, Pereira FV, Figueiredo CR, Matsuo AL, *et al*. Beta-actin-binding complementarity-determining region 2 of variable heavy chain from monoclonal antibody c7 induces apoptosis in several human tumor cells and is protective against metastatic melanoma. J Biol Chem 2012;287:14912-22.
30. Matsuo AL, Figueiredo CR, Arruda DC, Pereira FV, Scutti JA, Massaoka MH, *et al*. Alpha-Pinene isolated from Schinus terebinthifolius Raddi (Anacardiaceae) induces apoptosis and confers antimetastatic protection in a melanoma model. Biochem Biophys Res Commun 2011;411:449-54.
31. Balonov K, Khodorova A, Strichartz GR. Tactile allodynia initiated by local subcutaneous endothelin-1 is prolonged by activation of TRPV-1 receptors. Exp Biol Med (Maywood) 2006;231:1165-70.
32. Kwon YH, Jung SY, Kim JW, Lee SH, Lee JH, Lee BY, *et al*. Phloroglucinol inhibits the bioactivities of endothelial progenitor cells and suppresses tumor angiogenesis in LLC-tumor-bearing mice. PLoS One 2012;7:e33618.
33. Suzuki T, Shimizu T, Yu HP, Hsieh YC, Choudhry MA, Schwacha MG, *et al*. Tissue compartment-specific role of estrogen receptor subtypes in immune cell cytokine production following trauma-hemorrhage. Appl Physiol 2007;102:163-8.
34. Park D, Bae DK, Jeon JH, Lee J, Oh N, Yang G, *et al*. Immunopotentiation and antitumor effects of a ginsenoside Rg (3)-fortified red ginseng preparation in mice bearing H460 lung cancer cells. Environ Toxicol Pharmacol 2011;31:397-405.
35. Moreira IC, Lago JH, Young MC, Roque NF. Antifungal aromadendrane sesquiterpenoids from the leaves of Xylopia brasiliensis. J Braz Chem Soc 2003;14:828-31.
36. Moreira IC, Roque NF, Contini K, Lago JH. Sesquiterpenos e hidrocarbonetos dos frutos de Xylopia emarginata (Annonaceae). Rev Bras Farmacogn 2007;17:55-8.
37. Moreira CG, Horinouchi CD, Souza-Filho CS, Campos FR, Barison A, Cabrini DA, *et al*. Hyperpigmentant activity of leaves and flowers extracts of Pyrostegia venusta on murine B16F10 melanoma. J Ethnopharmacol 2012;141:1005-11.
38. Mates JM, Sanchez-Jimenez FM. Role of reactive oxygen species in apoptosis: implications for cancer therapy. Int J Biochem Cell Biol 2000;32:157-70.
39. Hengartner MO. The biochemistry of apoptosis. Nature 2000;407:770-6.
40. Zuo Y, Xiang B, Yang J, Sun X, Wang Y, Cang H, *et al*. Oxidative modification of caspase-9 facilitates its activation via disulfide-mediated interaction with Apaf-1. Cell Res 2009;19:449-57.
41. Liu SX, Davidson MM, Tang X, Walker WF, Athar M, Ivanov V, *et al*. Mitochondrial damage mediates genotoxicity of arsenic in mammalian cells. Cancer Res 2005;65:3236-42.
42. Jiang X, Wang X. Cytochrome c promotes caspase-9 activation by inducing nucleotide binding to Apaf-1. J Biol Chem 2000;275:31199-203.
43. Gottlieb E, Armour SM, Harris MH, Thompson CB. Mitochondrial membrane potential regulates matrix configuration and cytochrome c release during apoptosis. Cell Death Differ 2003;10:709-17.
44. Giammarioli AM, Maselli A, Casagrande A, Gambardella L, Gallina A, Spada M, *et al*. Pyrimethamine induces apoptosis of melanoma cells via a caspase and cathepsin double-edged mechanism. Cancer Res 2008;68:5291-300.
45. Kim BM, Choi YJ, Han Y, Yun YS, Hong SH. N, N-dimethyl phytosphingosine induces caspase-8-dependent cytochrome c release and apoptosis through ROS generation in human leukemia cells. Toxicol Appl Pharmacol 2009;239:87-97.
46. Sato T, Machida T, Takahashi S, Iyama S, Sato Y, Kuribayashi K, *et al*. Fas-mediated apoptosome formation is dependent on reactive oxygen species derived from mitochondrial permeability transition in Jurkat cells. J Immunol 2004;173:285-96.
47. Kumar S. Caspase 2 in apoptosis, the DNA damage response and tumour suppression: Enigma no more? Nat Rev Cancer 2009;9:897-903.
48. Zhivotovsky B, Orrenius S. Caspase-2 function in response to DNA damage. Biochem Biophys Res Commun 2005;331:859-67.
49. Prasad V, Chandele A, Jagtap JC, Sudheer KP, Shastry P. ROS-triggered caspase 2 activation and feedback amplification loop in beta-carotene-induced apoptosis. Free Radic Biol Med 2006;41:431-42.
50. Pietenpol JA, Stewart ZA. Cell cycle checkpoint signaling: Cell cycle arrest versus apoptosis. Toxicology 2002;181-182:475-81.
51. Ostrakhovitch EA, Cherian MG. Role of p53 and reactive oxygen species in apoptotic response to copper and zinc in epithelial breast cancer cells. Apoptosis 2005;10:111-21.
52. Suffness M, Pezzuto JM. Assays Related to Cancer Drug Discovery. In: Hostettmann K, editor. Methods in Plant Biochemistry: Assays for Bioactivity. London: Acad. Press; 1990. p. 71-133.
53. Krishna V, Sharma S, Pareek RB, Singh P. Terpenoid constituents from some indigenous plants. J Indian Chem Soc 2002;79:550-2.
54. Roy P, Amdekar S, Kumar A, Singh V. Preliminary study of the antioxidant properties of flowers and roots of Pyrostegia venusta (Ker Gawl) Miers. BMC Complement Altern Med 2011;11:69.
55. Takahashi C, Kikuchi N, Katou N, Miki T, Yanagida F, Umeda M. Possible anti-tumour-promoting activity of components in Japanese soybean fermented food, Natto: Effect on gap junctional intercellular communication. Carcinogenesis 1995;16:471-6.
56. Olubunmi A, Olatunji AG. Epicuticular wax and volatiles of *kigelia pinnata* leaf extract. Ethno leaflets 2010;14:797-806.

57. Dzhambazov B, Daskalova S, Monteva A, Popov N. *In vitro* screening for antitumour activity of Clinopodium vulgare L. (Lamiaceae) extracts. Biol Pharm Bull 2002;25:499-504.
58. Gomez-Flores R, Quintanilla-Licea R, Verde-Star MJ, Morado-Castillo R, Vazquez-Diaz D, Tamez-Guerra R, *et al*. Long-chain alkanes and ent-Labdane-type diterpenes from Gymnosperma glutinosum with cytotoxic activity against the murine lymphoma L5178Y-R. Phytother Res 2012;26:1632-6.
59. Moon SH, Jenkins CM, Liu X, Guan S, Mancuso DJ, Gross RW. Activation of mitochondrial calcium-independent phospholipase A2gamma (iPLA2gamma) by divalent cations mediating arachidonate release and production of downstream eicosanoids. J Biol Chem 2012;287:14880-95.
60. Amer WM, Abouwarda AM, El Garf IA, Dawoud GT, Abdelmohsen G. Phytochemical composition of *Solanum elaeagnifolium cav*. And its antibacterial activity. Int J Bio Pha Ali Sci (IJBPAS) 2013;2:1282-306.
61. Ghosh R, Banerjee S, Chakrabarty S, Bagchi B. Anomalous behavior of linear hydrocarbon chains in Water -DMSO binary mixture at low DMSO concentration. J Phys Chem 2011;B115:7612-20.
62. Capriotti K, Capriotti JA. Dimethyl sulfoxide: History, chemistry, and clinical utility in dermatology. J Clin Aesthet Dermatol 2012;5:24-6.
63. Stoughton RB, Fritsch W. Influence of dimethylsulfoxide (dmso) on human percutaneous absorption. Arch Dermatol 1964;90:512-7.
64. Goldmann L, Igelman JM, Kitzmiller K. Investigative studies with DMSO in dermatology. Ann N Y Acad Sci 1967;141:428-36.
65. Coldman MF, Kalinovsky T, Poulsen BJ. The *in vitro* penetration of fluocinonide through human skin from different volumes of DMSO. Br J Dermatol 1971;85:457-61.
66. Manjunath P, Shivaprakash BV. KrishiVigyan Kendra, Aland road, Gulbarga, UAS, Raichur, Karnataka. Pharmacology and Clinical Use of Dimethyl Sulfoxide (DMSO): A Review. Int J Mol Vet Res 2013;3:23-33.
67. Scherbel AL, McCormack LJ, Layle JK. Further observations on the effect of dimethyl sulfoxide in patients with generalized scleroderma. (Progressive systemic sclerosis). Ann N Y Acad Sci 1967;141:613-29.
68. Balonov K, Khodorova A, Strichartz GR. Tactile allodynia initiated by local subcutaneous endothelin-1 is prolonged by activation of TRPV-1 receptors. Exp Biol Med 2006;231:1165-70.
69. Suzuki T, Shimizu T, Yu HP, Hsieh YC, Choudhry MA, Schwacha MG, *et al*. Tissue compartment-specific role of estrogen receptor subtypes in immune cell cytokine production following trauma-hemorrhage. Appl Physiol 2007;102:163-8.
70. Kwon YH, Jung SY, Kim JW, Lee SH, Lee JH, Lee BY, *et al*. Phloroglucinol inhibits the bioactivities of endothelial progenitor cells and suppresses tumor angiogenesis in LLC-tumor-bearing mice. PLoS One 2012;7:e33618.
71. Ireland DJ, Greay SJ, Hooper CM, Kissick HT, Filion P, Riley TV, *et al*. Topically applied Melaleucaalternifolia (tea tree) oil causes direct anti-cancer cytotoxicity in subcutaneous tumour bearing mice. J Dermatol Sci 2012;67:120-9.

Cite this article as: Figueiredo CR, Matsuo AL, Pereira FV, Rabaca AN, Farias CF, Girola N, *et al*. Pyrostegia venusta heptane extract containing saturated aliphatic hydrocarbons induces apoptosis on B16F10-Nex2 melanoma cells and displays antitumor activity *in vivo*. Phcog Mag 2014;10:363-76.

Source of Support: Nill, **Conflict of Interest:** None declared.